Journal of Applied Polymer Science

# Bioactive polymeric nanofiber matrices for skin regeneration

**Eross Guadalupe,[1] Daisy Ramos,[2,3,4,5] Namdev B. Shelke,[2,3,4] Roshan James,[2,3,4] Christian Gibney,[1] Sangamesh G. Kumbar[2,3,4,5]**

[1]Department of Biomedical Engineering, University of Connecticut, Connecticut 06269
[2]Institute for Regenerative Engineering, University of Connecticut Health Center, Connecticut 06030
[3]The Raymond and Beverly Sackler Center for Biomedical, Biological, Physical and Engineering Sciences, Connecticut 06030
[4]Department of Orthopaedic Surgery, University of Connecticut Health Center, Connecticut 06030
[5]Department of Materials Science and Engineering, University of Connecticut, Connecticut 06269
E. Guadalupe and C. Gibney are BME Undergraduate Senior Design Students.
Correspondence to: S. G. Kumbar (E-mail: Kumbar@uchc.edu)

**ABSTRACT:** Electrospun nanofiber matrices have attracted a great deal of attention as matrices for skin repair and regeneration. The current manuscript reports the fabrication and characterization of a bioactive polycaprolactone (PCL) fiber matrix for its ability to deliver multiple factors. Bioactive PCL matrices were created by incorporating a model angiogenic factor and a model antibiotic drug. Chitosan coating on the fiber matrices significantly improved the ability to hold moisture and contributed to antibiotic activity. These fiber matrices have a modulus of $5.8 \pm 1.3$ MPa and matrices subjected to degradation over 4 weeks did not lose their tensile properties due to slow degradation rate. Chitosan coating avoided the initial burst release commonly associated with fiber matrices and only 60% of the encapsulated drug was released over a period of 15 days. Control PCL-chitosan matrices were able to reduce *Staphylococcus aureus* (*S. aureus*) growth both in static and dynamic condition as compared to formulations with 50 mg gentamicin. In general, all the fiber matrices were able to support fibroblast growth and maintained normal cell morphology. Such bioactive bandages may serve as versatile and less expensive alternatives for the treatment of complex wounds. © 2015 Wiley Periodicals, Inc. J. Appl. Polym. Sci. **2015**, *132*, 41879.

**KEYWORDS:** biodegradable; biomedical applications; drug delivery systems; fibers; nanostructured polymers

Received 22 October 2014; accepted 19 December 2014
**DOI: 10.1002/app.41879**

## INTRODUCTION

Every year, over 6.5 million people in the United States are affected with chronic wounds, amounting to 25 billion dollars in medical costs.[1,2] Chronic wounds, defined as wounds that do not heal within the normal time frame of 8–12 weeks, are complex abnormal wounds such as surgical wounds, diabetic ulcers, burns, and wounds due to other diseases.[3] The concern for better treatment of chronic wounds is due in part to the rising numbers of obesity and diabetes cases in the United States, along with an increase in aging population.[2] In addition, the necessity for better treatment of acute wounds is becoming more imperative with the occurrence of injuries caused by war, natural disasters, and unwarranted violence.[2] Both chronic and acute wounds can be complex in nature as the wounds extend beyond the epidermis layer and into the dermis and deeper layers, potentially affecting blood vessels, sweat glands, and hair follicles.[4]

The global market for wound care was valued at about 15.6 billion dollars in 2014[5] and is expected to grow in the coming years with emphasis on advanced wound dressings.[5,6] Proper treatment requires an understanding of the wound healing process.[3] The basic phases of wound healing include (1) inflammation, (2) proliferation (tissue formation), and (3) maturation (tissue remodeling). During the inflammatory stage, increased vasodilation with increased capillary permeability allows for the infiltration of leukocytes to the wound site. Platelet formation begins bringing along essential proteins such as growth factors that act as regulatory agents in wound healing. During the proliferative phase, fibroblasts proliferate at the wound site and begin to synthesize collagen fibers. During this phase, angiogenesis, the formation of new blood vessels, occurs in order to provide capillary growth into the wound site. The lack of capillary growth reduces the supply of oxygenated blood at the wound site, thus making an unfavorable environment for cells and negatively affecting the wound healing process. Finally, during the maturation phase, collagen fibers become more organized and reach normal skin ratios of 4 : 1 of type I : type III collagen content.[7] Improper treatment leads to infection,

unsightly scar tissue and in the case of chronic wounds, repeated injuries.

Complex wounds require treatment strategies beyond the traditional functions of conventional dressings that simply act to provide a barrier against infection. Traditional dressings do very little to expedite healing and may even be detrimental as they can potentially remove healing cells during replacement.[8] Today, it is well understood that maintaining a moist environment in the wound bed provides for better healing. Most dressings are now made from synthetic polymeric materials and much research is focused on the addition of bioactive factors for enhanced healing.[3] Advanced bioactive dressings are equipped with antimicrobial properties, minimize scar formation, and promote faster healing.

Electrospun fiber matrices act as engineered skin substitutes that are widely researched as bioactive dressings.[9–14] Electrospinning is a common fabrication technique extensively used in tissue engineering applications utilizing a high voltage source to create fibers with diameters in the micrometer and nanometer range.[14,15] The advantages of these electrospun fibers lay in their simplistic fabrication process, versatility, and their close resemblance to the natural extracellular matrix of cells that help promote cellular adhesion and proliferation.[9] Moreover, the high surface area to volume ratio of these fiber matrices allows for greater cell attachment and better contour to injuries with higher surface area for wound contact.

Nanofibrous matrices can act as delivery vehicles for cells, drugs, proteins, small molecules, or other therapeutic agents.[16,17] Angiogenic growth factors such as platelet-derived growth factor, vascular endothelial growth factor (VEGF), epidermal growth factor (EGF), and others have been incorporated into electrospun polymers which aid in the regeneration of damaged human skin.[18–20] Poly(lactide-co-glycolide) (PLGA) nanofiber-based systems have also been used to deliver and administer antibiotics to wound sites.[21]While advanced dressings have noticeable benefits to wound healing and recovery, the resources to produce and manufacture these dressings come at a high financial cost. Growth factors incorporated into the dressings can cost up to hundreds of dollars for nanogram quantities. In addition, growth factors are susceptible to degradation during electrospinning and sterilization processes and require large physiological doses to be effective in the body.[22]

To overcome the limitations associated with growth factors, researchers are directing efforts toward the discovery of small molecules as alternatives to growth factors. Small molecules (<5 kDa) have diffusion coefficients an order of magnitude greater than large proteins[23] thereby making small molecules better suited for localized drug delivery applications.[24] In addition, small molecules may survive encapsulation and sterilization processes better than peptide-based growth factors,[24] which have been shown to undergo degradation during fabrication.[22] A small molecule phthalimide neovascular factor-1 (PNF1) (Figure 1) (CAS#: 10442-95-2; M.P. 175–177°C, B.P. 393.5°C, pKa value: $-2.45 \pm 0.2$, Solubility: water, methanol) has been reported to show angiogenic effects similar to VEGF.[25,26] This molecule is reported to maintain its structure and bioactivity

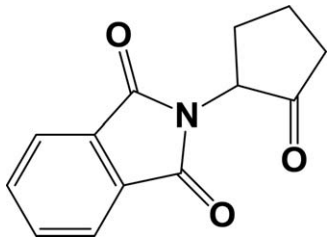


**Figure 1.** Chemical Structure of phthalimide neo-vascular factor 1 (PNF1).[24]

even after exposure to ultraviolet irradiation and encapsulation in polymeric matrices using chlorinated solvents. PNF1 released from polymeric matrix retained its bioactivity and improved the survival rate of endothelial cells.[24–26]

This study reports the fabrication and characterization of bioactive polycaprolactone (PCL) nanofiber matrices incorporated with a model angiogenic factor, PNF1 and a model antibiotic drug, gentamicin. It was hypothesized that coating drug loaded nanofiber matrices with a chitosan layer will avoid the initial burst and provide sustained drug release over a period of time as compared to nanofiber matrices alone. It was also hypothesized that a chitosan layer may help to retain moisture at the wound site while providing additional antimicrobial properties. Studies were conducted to evaluate the drug diffusion rates, cell compatibility, and antimicrobial properties.

## MATERIALS AND METHODS

### Materials

Potassium phthalimide salt and 2-chlorocyclopentanone were purchased from Sigma Aldrich (St. Louis, MO) to synthesize PNF1 according to published literature report.[24] PCL (80,000 Mw), hydrochloric acid (HCL), dimethylformamide (DMF), methylene chloride (MC), and gentamicin sulfate were purchased from Sigma Aldrich. Chitosan used in this study was obtained from ICO Polymers (Allentown, Pennsylvania). Human skin fibroblasts (hSkF) and Eagle's minimum essential medium (EMEM) were purchased from ATCC. Fetal bovine serum, antibiotics (Penicillin, Streptomycin P/S), and trypsin-EDTA were purchased from Life Technologies (Grand Island, NY). All other reagents and materials were used without further purification.

### Synthesis of PNF1

The synthesis of PNF1 was carried out as per previously published literature. In brief, a mixture of potassium phthalimide salt (3 g, 10.8 m*M*) and 2-chlorocyclopentanone (2 g, 12.96 m*M*) was stirred in a reaction vessel at 60°C for 3 h under nitrogen atmosphere using 8 mL of DMF as a solvent.[24] The solution was precipitated in ice water and collected by vacuum filtration and freeze-dried overnight (LabConco, Kansas City, MO). The crude brown solid was then purified via column chromatography with 50/50 hexane/ethyl acetate to yield ~12% PNF1 of white powder solid.

### Electrospinning of PCL/PNF1 Matrices

Drug loaded nanofiber matrices were fabricated using standard electrospinning set-up by solution co-spinning.[14] A 15% (w/v)

**Table I.** Antibiotic Drug Gentamicin Eluting Nanofiber Matrix Formulations

| Chitosan solution concentration % (wt/v) | % Gentamicin loading (dry weight of chitosan) |
|---|---|
| 4 | 5 |
| 4 | 10 |
| 4 | 15 |
| 5 | 5 |
| 5 | 10 |
| 5 | 15 |
| 6 | 5 |
| 6 | 10 |
| 6 | 15 |

PCL solution was prepared in a solvent mixture comprised of MC and DMF at a ratio of 3 : 1. A 5 wt % of PNF1 was added to PCL solution and mixed well prior to electrospinning. A 6 mL volume of the above polymer solution was placed in a 10 mL syringe with an 18G needle and electrospun at 20 kV at a rate of 4 mL/h with a working distance of 15 cm. The selection of PNF1 concentration was based on previous literature reports.[26] A series of chitosan solutions between 4 and 6% (w/v) in 1% aqueous HCL were prepared to coat the drug loaded nanofiber matrices. These nanofiber matrices were then dipped into the chitosan solution for 3 s at a time to allow a thin uniform coating and allowed to dry. The selected coating parameters to achieve a uniform and reproducible coating on the fiber matrices was based on our previous work published elsewhere.[27]

### Nanofiber Matrices Coating with Chitosan/Gentamicin

A series of chitosan solutions between 1.5 and 2.5% (w/v) in 1% aqueous HCL were prepared as coating solutions. Varying amounts of gentamicin between 5 and 15% (w/v) of the dry weight of chitosan was added to the coating solutions to produce nine different formulations presented in Table I. The electrospun nanofiber matrices were then dip coated using the method described above.

### Bioactive Molecule Entrapment Efficiencies of Nanofiber Matrices

**PNF1 Entrapment Efficiencies.** The weighed amount of PNF1 loaded nanofiber matrix was dissolved in 2 mL of a solvent mixture comprised of MC and DMF at a ratio of 3 : 1. To this solution, 5 mL of DI water was added to precipitate the polymer. The drug containing solution was filtered using a syringe filter and the volume of the solution was adjusted to 10 mL with DI water. The concentration of PNF1 was measured using UV-spectrophotometer at 405 nm using a standard curve created in a same solvent composition. For these measurements, three different samples were used and average encapsulation efficiencies were reported.

**Gentamicin Entrapment Efficiencies.** The weighed amount of nanofiber matrices coated with chitosan and gentamicin were incubated in 5 mL of DI water containing 1 vol % HCl solution for 1 h. Dissolved chitosan was precipitated by adding the 1*N* sodium hydroxide (NaOH) solution. Drug containing aqueous solution was filtered using a syringe filter to separate PCL and chitosan. The filtrate volume was adjusted to 10 mL using DI water. The concentration of gentamicin was measured using the o-pthalaldehyde (OPA) assay as outlined in the following section.[28] For these measurements, three different samples were used and average encapsulation efficiencies were reported.

The encapsulation efficiencies of PNF1 and gentamicin were calculated using the following equation.

$$\text{Drug loading efficiencies} = (\text{Actual drug loading}/\text{Theoretical drug loading}) \times 100$$

### Mechanical Characterization

Mechanical properties of the PCL matrices were determined using a mechanical tester (Instron 5544, Norwood MA). The samples were cut into dog-bone shapes with the test section being 20 × 10 $mm^2$ (length × breadth) according to American Society for Testing and Materials (ASTM) standards.[29] These samples were incubated in phosphate buffer saline (PBS, pH 7.4) at 37°C for a 4-week period and wet samples were tested at time points of 1, 2, 3, and 4 weeks. These specimens were stretched at constant speed of 10 mm/min to failure and a sample size of $n = 6$ were used for each time point.

### *In Vitro* Drug Release from Fiber Matrices

**PNF1 Release Characterization.** Due to the lack of a UV chromophore in PNF1, often p-nitroaniline (PNA, FW = 138.12) has been used as a surrogate molecule to quantify the PNF1 release.[26] To facilitate these quantifications PCL/PNA nanofiber matrices were fabricated using similar electrospinning parameters and concentrations used for PNF1 encapsulation, and coated with chitosan. These matrices were cut into circular discs using cork-borer no. 10 with an area of approximately 2.27 $cm^2$ and a thickness of 0.45–0.52 mm and incubated at 37°C in 2.0 mL solution of 1× PBS in a 24 well plate. The dissolution media was collected and replaced daily for 15 days. The absorbance of PNA was quantified using UV/Vis spectrophotometer at 405 nm from which the concentration was calculated using a standard curve. For all these release studies a sample size of $n = 3$ were used.

**Gentamicin Release Characterization.** Fiber matrices coated with chitosan solutions containing gentamicin were cut into circular discs as explained above and incubated at 37°C in 2.0 mL solution of 1× PBS in a 24 well plate. The dissolution media was collected and replaced daily for 15 days and was analyzed for gentamicin content using the OPA reagent method.[28] The reagent OPA reacts with primary amines to produce a fluorescent compound that can be excited at 360 nm and detected at 465 nm using a UV/Vis spectrophotometer. Approximately 300 µL of the complete solution of OPA (Sigma Aldrich), already containing $\beta$-mercaptoethanol and boric acid, was added to 10 µL of each sample and the reaction solution was incubated for 5 min. Following the 5 min, the sample fluorescence was read using a UV/Vis spectrophotometer. First, a calibration was performed to determine the fluorescence intensity for given dilution series of gentamicin. A standard curve ($y = 66.61x + 10443$, $R^2 = 0.935$) was constructed; and, the

concentration of gentamicin released at specific time points was extrapolated from the slope of the standard curve. The amount of antibiotic released was reported in terms of micrograms (μg). For all these release studies a sample size of $n = 3$ were used.

### Sorption Experiments

Dynamic and equilibrium swelling experiments on the fiber matrices coated with chitosan were performed in PBS at 37°C. The initial mass of circular discs of fiber matrices ($W_o$) were noted using a single pan digital microbalance (Mettler Toledo) sensitive to ±0.01 mg. Fiber matrices were incubated at 37°C in 2.0 mL solution of 1× PBS in a 24 well plate. At various time intervals samples were removed from the wells, excess of the water adhered to the surface was removed by gently pressing them between filter papers and corresponding mass was noted ($W_t$). Sorption data obtained at different time intervals was used to calculate % mass uptake ($M_t$) using the following equation. For all these studies a sample size of $n = 3$ were used.

$$M_t = \frac{W_t - W_o}{W_o} \times 100$$

### Quantification of Antimicrobial Properties

Fiber matrices coated with chitosan, with and without gentamicin, were tested for antimicrobial properties under static and dynamic conditions using *Staphylococcus aureus* strain. It is the most commonly found bacterium on the skin. Fiber matrices (PCL-chitosan) containing 50, 100, 150 mg of gentamicin were tested and results were compared with PCL and PCL-chitosan control fiber matrices. The static test is an agar diffusion test in which microbial growth inhibition zone around the circular fiber matrices were measured and presented in diameters of clear zones.[30] Fiber matrices were placed in agar plates and incubated for 24 h at 37°C and the zone of inhibition for each sample was measured using calipers. For all these studies a sample size of $n = 3$ were used.

One set of fiber matrices were incubated in 2 mL of PBS at 37°C and 250 μL of this release media was collected at various time points up to 15 days. The bioactivity of the released gentamicin was tested in dynamic condition by adding this media to bacterial suspension with known absorbance and recording its changes. In brief, 250 μL release media was added to 750 μL *S. aureus* suspension in tryptic soy broth media and incubated at 37°C for 30 min. Using a UV/Vis spectrophotometer, the changes in absorbance at 600 nm were measured at 0.5, 1, 2, and 4 h and later time points at 3, 9, and 15 days. The reduction in the absorbance value is the indication of decrease in the concentration of bacterial suspension. For all these studies a sample size of $n = 3$ were used.

### Cell Proliferation (Quant-iT™ PicoGreen dsDNA assay)

Circular discs of fiber matrices in both test and control groups were sterilized by immersing matrices in 70% ethanol for 20 min followed by exposing to UV light for 1 h on each side. Scaffolds were placed in 24 well plates and washed by soaking completely in serum supplemented EMEM for 15 min to remove traces of alcohol. Each matrix was seeded with 50,000 cells and 1.8 mL of growth media was added to the samples and then changed completely every other day. The cell proliferation on the surface of the non-woven fiber matrices was quantified by measuring the amount of cellular DNA content using PicoGreen dsDNA assay (P7589, Life Technologies) at 3, 7, and 10 day time points. At the end of each time point, cellular constructs were washed twice with PBS, transferred to new well plates, and 1 mL of 1% Triton X-100 was added to lyse the cells and samples were then stored in −20°C until further analysis. Prior to the analysis the well plates underwent three freeze–thaw cycles, and the contents were thoroughly mixed with the aid of a pipette to extract cell lysate. Ten microliters of sample DNA was transferred into a new well plate to which 90 μL (component B) and 100 μL (Component A) kit reagents were added. Well plates were covered with aluminum foil to prevent light exposure and incubated for 5 min. A BioTek plate reader was used to measure fluorescence (ex/em 485/535 nm). Optical readings were converted to cell numbers using a standard curve. The absorbance produced by the DNA extracts of five known cell numbers 10,000, 20,000, 40,000, 85,000, and 120,000 were used to construct a standard curve to convert absorbance readings to cell numbers. For all these studies a sample size of $n = 4$ were used.

### Field Emission Scanning Electron Microscopy

Field emission scanning electron microscopy (FESEM) was used to qualitatively access fiber matrix morphology and cell spreading on these matrices at various time points. In brief, cellular constructs harvested at various time points were collected, washed with PBS (pH 7.4), and fixed with 3% glutaraldehyde/paraformaldehyde overnight and washed with water, dried, and kept desiccated. Scaffold surfaces were sputter coated with Au/Pd using a Hummer V sputtering system (Technics, Baltimore, MD) prior to imaging.[31] Images were taken at various magnifications using a JEOL 6335F FESEM operated at an accelerating voltage of 15 kV.

### Confocal Microscopy

Live/Dead Assay Kit (L3224, Invitrogen) was used to visualize live and dead cells using confocal microscopy at various cell culture points. Cellular constructs were washed twice with warm PBS and then incubated with calcein-AM (2 $\mu$M) and ethidium homodimer-1 (EthD-1, 4 $\mu$M) and viewed under confocal microscopy using 10× magnification at ex/em: 494/517 nm (calcein-AM, green) and 528/617 nm (ethidium homodimer-1, red). In brief, calcein AM enters live cells and reacts with intracellular esterase to produce a bright green fluorescence, while ethidium homodimer-1 enters only dead cells with damaged membranes and produces a bright red fluorescence upon binding to nucleic acids.[32]

### Statistical Analysis

Statistical significance was determined by student's *t*-test, analysis of variance, and Tukey's post hoc test multiple comparisons ($P < 0.05$) using GraphPad Prism™ software.

## RESULTS AND DISCUSSION

### Fabrication and Characterization of Bioactive Matrices

PNF1 was synthesized according to the published procedure elsewhere and structure was confirmed by FTIR and NMR spectroscopy.[24–26] Earlier reports incorporated PNF1 in PLGA microspheres and found that the release pattern obtained by 5% (w/w) PNF1 encapsulation promoted expansion and ingrowth of microvascular networks surrounding biomaterial

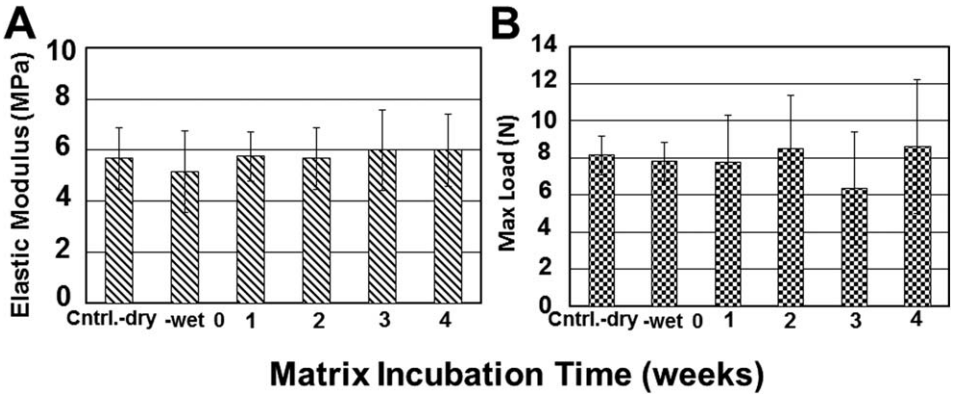


**Figure 2.** Tensile properties (A) Elastic modulus and (B) Maximum load for PCL nanofiber matrices over a period of 4 weeks in PBS at pH 7.4 and 37°C. There was no significant difference in tensile properties over a period of 4 weeks both in dry and wet conditions due to the slow degrading nature of PCL.

implants.[24–26] In our studies, a 5% (w/w) PNF1 was dissolved in PCL solution and fiber matrices were fabricated using optimized parameters. The drug loading efficiency for PNF1 was found to be 78.6 ± 8.3%. These values are similar to many nanofiber based drug delivery systems reported in the literature.[16] The lower encapsulation efficiencies are due to many factors including the charges carried by the bioactive molecules, solubility in electrospinning solvents, polymer system, and applied electrospinning parameters.[16] Matrices with PNF1 were found to have average fiber diameters of 273 nm ± 94 nm while neat PCL fibers at similar polymer concentration and parameters were found to be at 382 nm ± 140 nm. The reduced fiber diameters may be due to altered PCL solution parameters in terms of increased electrical conductivity of the polymer solution and surface change density of the fiber jet. Similar observations have been made with the addition of drugs or salts in other polymer systems.[16,33] Figure 2 presents the tensile properties of these fiber matrices tested at physiological pH and temperature up to 4 weeks. These fiber matrices showed a modulus of 5.8 ± 1.3 MPa and matrices did not lose their tensile properties over a period of 4 weeks in both dry and wet conditions due the slow degrading nature of PCL.[34]

Nanofiber matrices in general, release most of the encapsulated drug in the first few hours due to high surface area and enhanced drug solubility.[16] For instance, electrospun silk fibers encapsulated with EGF released majority of encapsulated EGF within the first 24 h.[4,17] In an effort to avoid this initial burst release and sustain the release up to 4 weeks, nanofiber matrices were coated with chitosan solution. Polysaccharide chitosan has been widely used for a variety of drug delivery and tissue regeneration applications.[12,30,35–37] In addition to excellent biocompatibility this polymer is known to exhibit antimicrobial properties, making it an attractive material for bioactive tissue engineering dressings.[30] A calculated amount of gentamicin, a model antibiotic drug, was dissolved in chitosan solution and used as a coating solution. The drug loading efficiencies for gentamicin were found to be 92.3 ± 6.2%. A total of nine different formulations were made and the details are provided in Table I. Increase in coating solution concentration and higher drug content would allow optimization of the bioactive factor release up to 4 weeks.

Hydration at the wound site is important in maintaining functionality and ability to release drugs.[4] Figure 3 represents water uptake characteristics of the fiber matrices. Chitosan coating significantly improved water retention capability and all the fiber matrices were able to attain equilibrium in the first 2 h. However, the higher water content on the chitosan coated membranes with drug beyond 2 h may result in additional water penetration into the voids created following drug diffusion. Coating chitosan on to PCL fiber matrix is a physical process and hence no chemical interactions were expected between PCL and chitosan. Chitosan coated fiber matrix was analyzed for molecular weight using gel permeation chromatography by dissolving the matrix in THF and undissolved chitosan was removed by filtration using a syringe filter. We did not observe any difference in molecular weights of the neat PCL fiber and chitosan coated fiber matrices (Mw ~ 80,000). Further FTIR measurements on the filtered PCL solution did not indicate any modifications to the PCL characteristic bands indicating the absence of chemical interactions between two polymers in presence of aqueous 1% (vol.) HCL. Figure 4 presents the PNA release profile from fiber matrices dip coated with 4%, 5%, and 6% chitosan solution. The PCL control fiber matrix alone

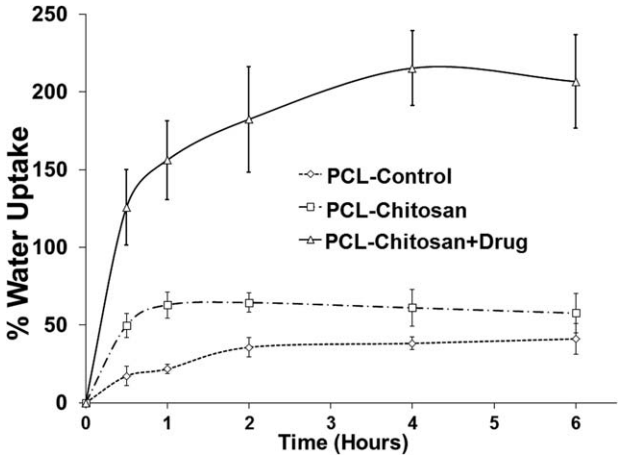


**Figure 3.** Water retention analysis showed nanofiber dressings containing model drug PNA were the most absorbent, followed by PCL-chitosan dressings and PCL alone fibers.

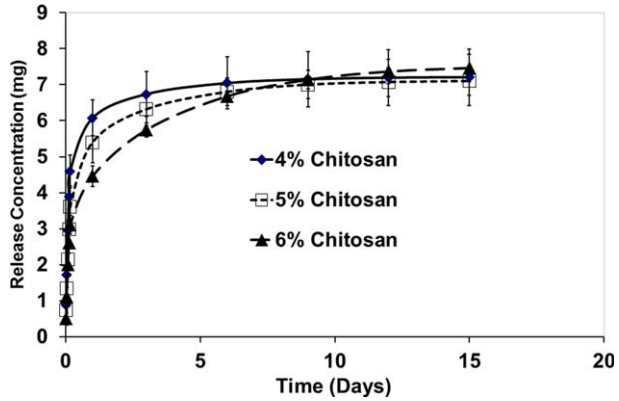


**Figure 4.** Release profile of model drug PNA from electrospun nanofibers dip coated with 4%, 5%, and 6% chitosan solution. All groups demonstrated a burst release of PNA within the first 24 h. However, PCL control fiber matrix alone lost the entire drug in the first 12 h. Fibers dip-coated with higher concentrations of chitosan showed a slower release of PNA demonstrating the ability to modulate drug release altering coating solution concentration. [Color figure can be viewed in the online issue, which is available at wileyonlinelibrary.com.]

released the entire drug loaded in the first 12 h. During the first 4 h, 4% dip coated samples had the highest release rate of the experimental samples. After Day 1, 6% dip coated samples had the least amount of PNA released, followed by 4% and followed by 5% dip coated samples ($P < 0.05$). There was no statistical difference among the samples after 24 h. This indicates that all samples displayed a burst release with a majority of the loaded PNA being eluted within the first 24 h. However 6% dip coated samples had a thicker coating of chitosan surrounding the fibers, resulting in a slower release of PNA and thus sustaining release throughout the 15 days tested. Figure 5 represents gentamicin release profile from PCL fiber matrices dip coated with 4%, 5%, and 6% chitosan solutions containing 5, 10, and 15% (w/w) concentrations of gentamicin. Fiber matrices dip-coated with higher concentrations of chitosan showed a slower release of gentamicin demonstrating the ability to modulate drug release through dip-coat concentration. These matrices were able to release 60% of the encapsulated drug over a period of 15 days. It is also evident that higher amount of gentamicin loading resulted in slower gentamicin release rate. The slower rate of drug diffusion at higher drug concentration may be due to the possible drug crystallization.[36,38]

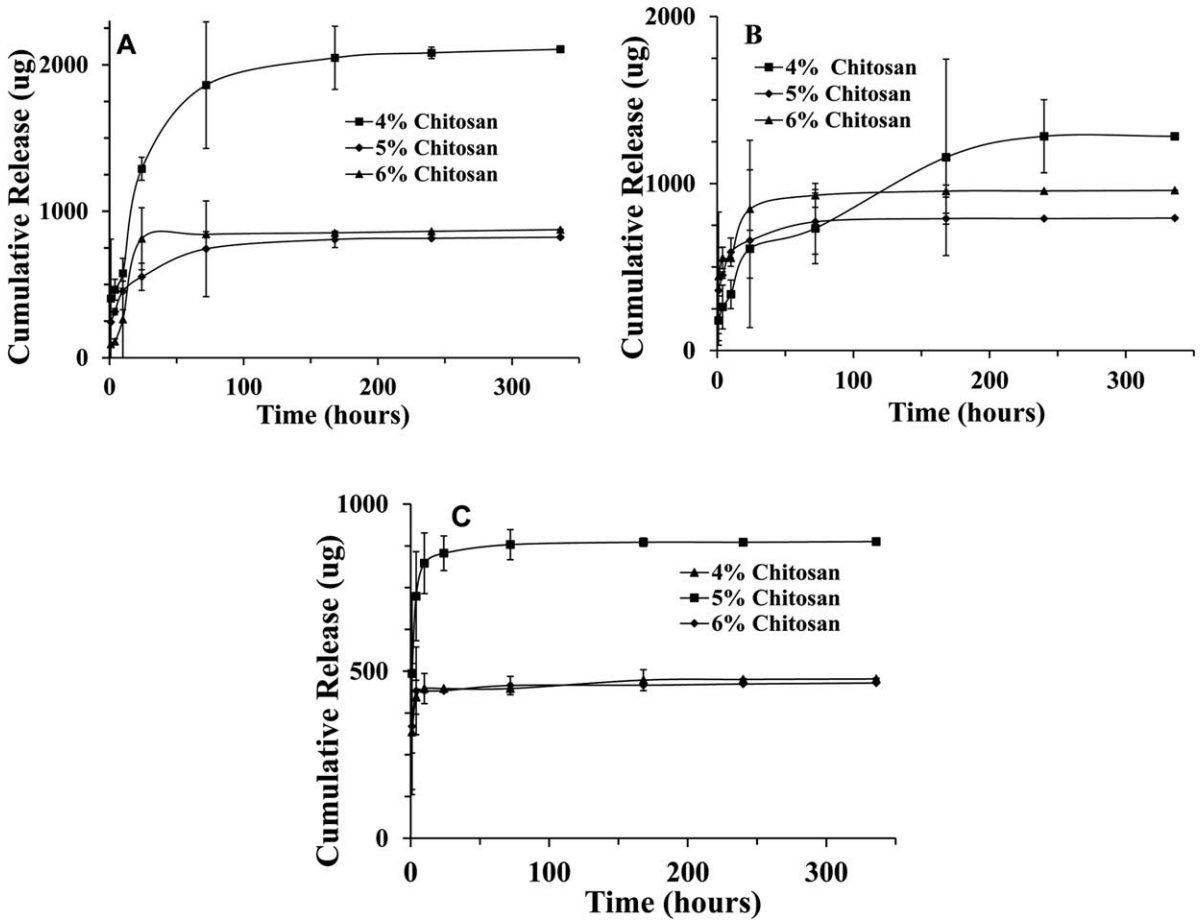


**Figure 5.** Release profiles of gentamicin from PCL nanofibers coated with 4%, 5%, and 6% chitosan solution containing (A) 5%, (B) 10%, and (C) 15% (dry weight of chitosan) gentamicin. In general fiber matrices coated with higher concentrations of chitosan showed a slower release of gentamicin due to the increased diffusional length. It is also evident that higher amount of gentamicin loading resulted in slower gentamicin release rate presumably due to crystallization at higher loading concentrations. These matrices were able to release 60% of the encapsulated drug over a period of 15 days.

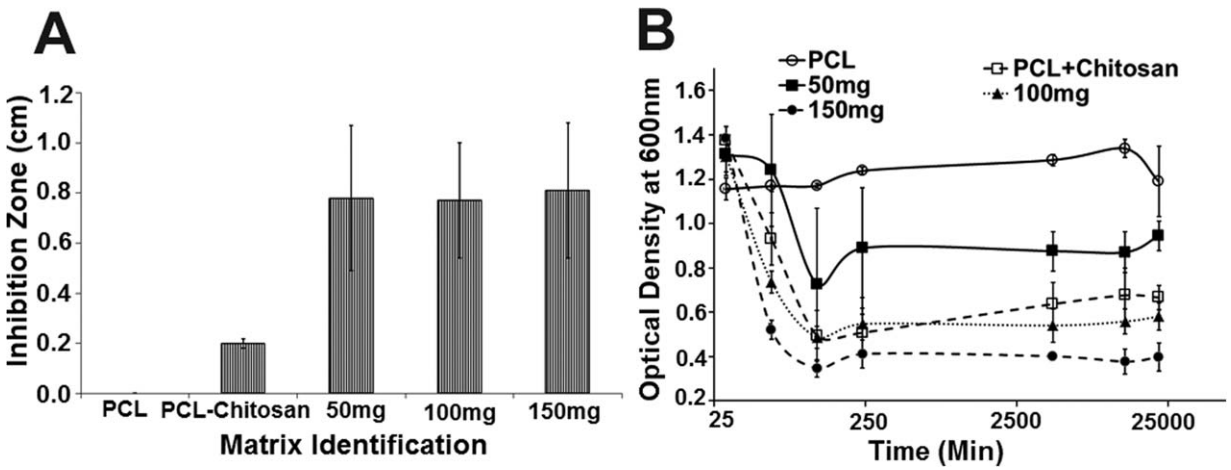


**Figure 6.** *In vitro* antimicrobial properties (A) In static *S. aureus* culture fiber matrices were incubated for 24 h at 37°C and inhibition zones (cm) were measured. Gentamicin containing matrices were significantly higher than control matrices, however, no statistical difference was found amongst samples with varying amounts of gentamicin. (B) Gentamicin efficacy following its release from the matrices was tested in dynamic condition and reduction in absorbance values was recorded at 0.5, 1, 2, and 4 h and at later time points 3, 9, and 15 days. In general gentamicin formulations and chitosan contributed to antimicrobial properties and were able reduce the bacterial growth. Control PCL-chitosan matrix showed lower bacterial levels as compared to formulations with 50 mg gentamicin.

### Antimicrobial Properties

An essential function of wound dressings is the ability to protect the open wound from infection by providing a physical barrier against bacteria.[39,40] Figure 6(A) presents the agar diffusion test which shows that the addition of gentamicin created a zone of inhibition. PCL matrix lacked *S. aureus* inhibition while chitosan coating showed moderate levels of antimicrobial properties. Gentamicin containing matrices exhibited a significantly higher zone of inhibition than control matrices, however, no statistical difference was found amongst samples with varying amounts of gentamicin. The results indicate that chitosan without the addition of gentamicin may not be sufficient as a dressing in preventing infections.

The dynamic antimicrobial test [Figure 6(B)] showed that gentamicin incorporated into the samples was bactericidal and absorbance of the bacterial media significantly dropped indicating less intact bacterial cells in the solution. All of the dip coated samples displayed a sharp drop in the bacterial absorbance after 2 h. The absorbance then started to gradually increase as the elution of gentamicin ceased after 4 h, indicating bacteria growth. Control PCL-chitosan matrix showed lower bacterial levels as compared to formulations with 50 mg gentamicin. Thus, 50 mg of gentamicin may not be an effective dose for minimizing bacteria growth. In addition, to reducing the number of dressing changes, a higher amount of gentamicin may be required to maintain bactericidal properties for longer than 4 h. Nevertheless, we have shown that the antibacterial property of gentamicin is conserved through the fabrication process.

### Skin Fibroblast Adhesion Proliferation and Viability

Bioactive dressings are made to interact with cells to accelerate wound healing through both physical and chemical cues.[14,15,29,41] Electrospun fibers due to their resemblance to the natural ECM, have been shown to affect cell growth and differentiation.[41] Human skin fibroblasts were seeded on electrospun nanofibers. The greatest number of cells were found on PCL and PCL/PNF1 scaffolds at all-time points (Figure 7). Matrices with chitosan coating had lower number of cells. At Day 3, there were significantly more cells on PCL/PNF1 scaffolds than PCL scaffolds which were later verified by SEM images shown in Figure 8(A,B). This is in line with previous research showing the effect of PNF1 on the proliferation of human microvascular endothelial cells (HMVEC) and Sarcoma osteogenic SaOS-2.[24] The addition of PNF1 in exogenous media led to a two fold increase in cell growth in HMVEC population within the first week and an 18-fold increase after 2 weeks. A relatively smaller increase was found with SaOS-2 cells. We found a two fold increase with PNF1 when compared to cells seeded on PCL scaffolds. The release profile of the model protein PNA,

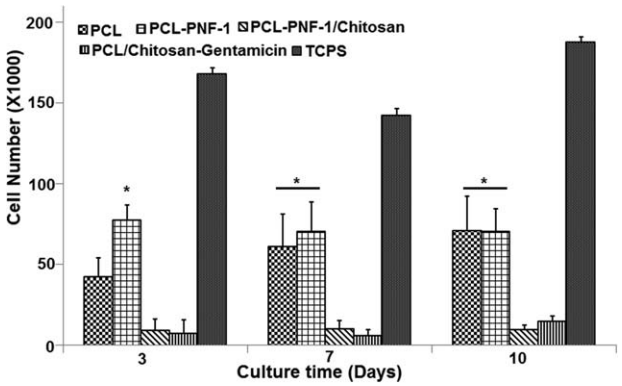


**Figure 7.** Proliferation of human skin fibroblasts cultured on fiber matrices over a period of 10 days post-seeding. At all the time points PCL matrices with and without PNF1 showed significantly higher cell number than chitosan coated fiber matrices with and without PNF1 or gentamicin. The steady cell proliferations on chitosan coated fiber matrices may be attributed to inefficient DNA extraction from the matrices or detachment of the cells during culture. In general all the fiber matrices were able to support fibroblast growth.

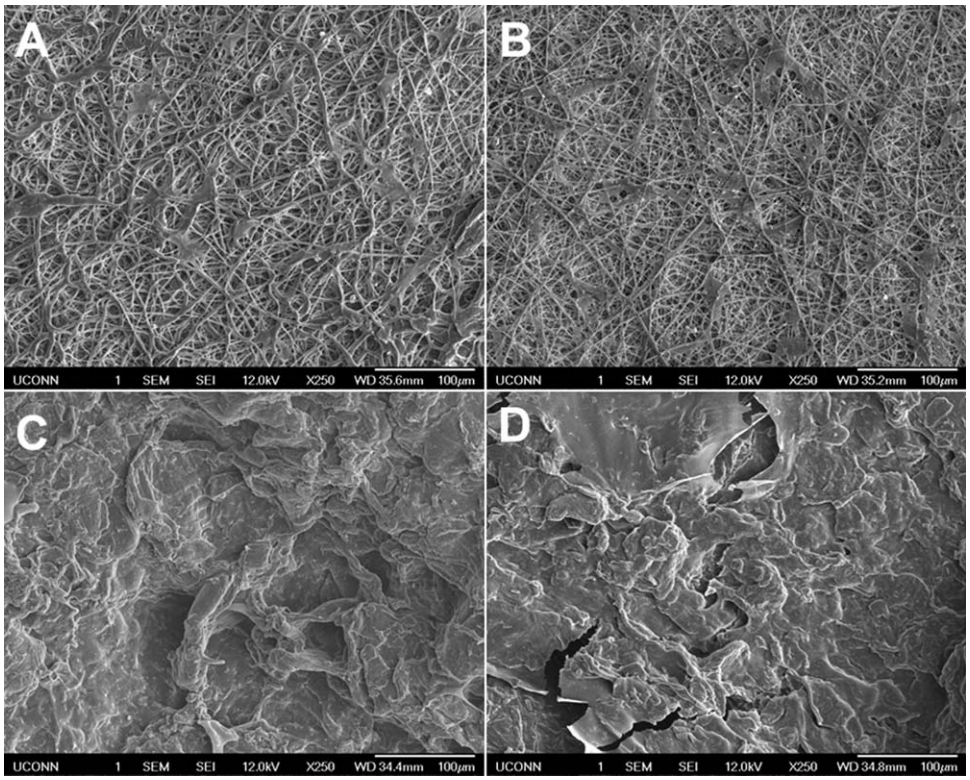


**Figure 8.** SEM micrographs of (A) PCL and (B) PCL-PNF1, (C) PCL-PNF1/chitosan and (D) PCL-chitosan-gentamicin showing human skin fibroblasts morphology at day 7 post-seeding. It was difficult to identify cells on the fiber matrices coated with chitosan due to the rough surfaces. In general cells were evident on the PCL and PCL-PNF1 matrices which were also supported by cell proliferation studies indicating more cells on these two matrices.

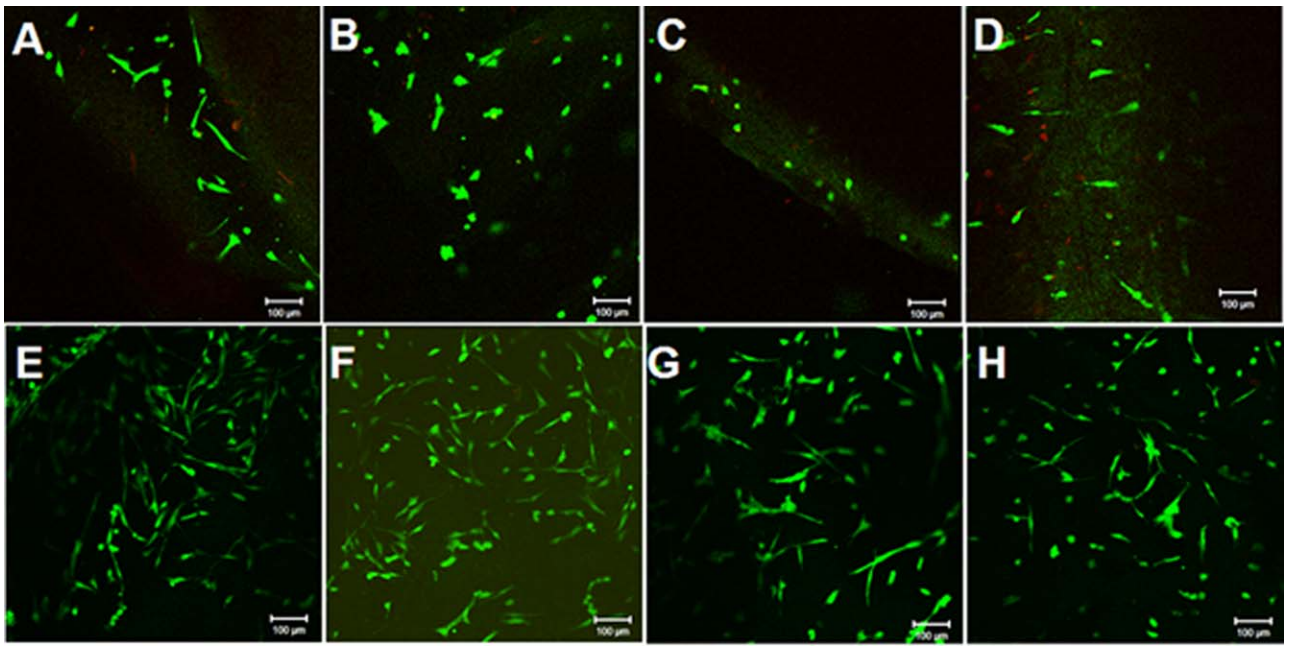


**Figure 9.** Confocal microscopy images of human skin fibroblast morphology and cell survival on chitosan coated PCL fiber matrices determined by viability/cytotoxicity assay. Live cells appear as fluorescent green color and dead cells as fluorescent red. Matrices on the top panel A-D represent PCL, PCL-4, PCL-5 and PCL-6% chitosan coated samples on day 3 post-seeding. The bottom panel represents the same set of samples at day 7 post-seeding. These matrices were able to support skin fibroblast growth and maintained a normal morphology. [Color figure can be viewed in the online issue, which is available at wileyonlinelibrary.com.]

indicated that majority of the molecule is eluted within the first 24 h, suggesting the effect of PNF1 on cell proliferation would not be seen at later time points as indicative of the lack of statistical significance found between PCL/PNF1 and PCL scaffolds at Day 7 and Day 10. DNA content on chitosan coated scaffolds was significantly less than neat PCL fiber matrices. The steady cell proliferations on chitosan coated fiber matrices may be attributed to inefficient DNA extraction from the matrices during assay or due to detachment of the cells during culture. Figure 8 represents the cell morphology on day 7 post seeding. In general cells were evident on the PCL and PCL-PNF1 matrices, which were also supported by cell proliferation studies indicating more cells on these two matrices. To support these arguments cell viability studies were done using a Live/Dead Assay kit. Live cells appear as fluorescent green color and dead cells as fluorescent red (Figure 9). Human skin fibroblasts on the fiber matrices coated with 4, 5, and 6% chitosan solutions at time points of 3 and 7 day post seeding are presented in Figure 9. These images allow identification of cells on the chitosan coated nanofiber matrices which was difficult from SEM micrographs presented in Figure 8. More than 90% viable cells were found on the chitosan coated fiber matrices at various culture points such as 1, 3, 7, and 14 days. These matrices were able support skin fibroblast growth and maintained a normal morphology. Higher cell number was seen on all the matrices on day 7 as compared to day 3 indicating cell survival. The SEM and confocal images indicate progressive cell growth on fiber matrices.

## CONCLUSIONS

Advanced wound healing dressings need to maintain a moist occlusive environment, prevent infections, absorb exudates, and promote cell growth. Though the benefits of bioactive dressings are recognized, their use is limited due to high associated costs with bioactive growth factors. Small molecule phthalimide neovascularization factor has previously been shown to increase proliferation of endothelial cells and promoted microvascular networks *in vivo*. The angiogenic effect of PNF1 makes it an ideal candidate for use in promoting vascularization in tissue engineering strategies. In this study, we have successfully electrospun PCL fibers with PNF1 to act as a bioactive dressing for wound healing applications. We have shown that electrospun PCL fibers with PNF1 are highly absorbent and demonstrate antibacterial properties when dip coated with chitosan and gentamicin. We present a simple method to encapsulate multiple factors and show the ability to deliver these factors up to 4 weeks to promote wound healing. This work has provided a proof of concept for a potentially low-cost bioactive dressing for wound healing applications. Current studies are underway to evaluate their wound healing efficacy in an animal model.

## ACKNOWLEDGMENTS

Funding for this research comes from the Raymond and Beverly Sackler Center for Biomedical, Biological, Physical and Engineering Sciences. Authors also acknowledge the funding from National Science Foundation Award Number IIP-1311907, IIP-1355327; and EFRI-1332329 as well as Department of Defense- OR120140.

## REFERENCES

1. Baquerizo Nole, K. L.; Yim, E.; Van Driessche, F.; Davidson, J. M.; Martins-Green, M.; Sen, C. K.; Tomic-Canic, M.; Kirsner, R. S. *Wound Repair Regen.* **2014**, *22*, 295.
2. Sen, C. K.; Gordillo, G. M.; Roy, S.; Kirsner, R.; Lambert, L.; Hunt, T. K.; Gottrup, F.; Gurtner, G. C.; Longaker, M. T. *Wound Repair Regen.* **2009**, *17*, 763.
3. Zahedi, P.; Rezaeian, I.; Ranaei-Siadat, S. O.; Jafari, S. H.; Supaphol, P. *Polym. Adv. Technol.* **2010**, *21*, 77.
4. Boateng, J. S.; Matthews, K. H.; Stevens, H. N.; Eccleston, G. M. *J. Pharm. Sci.* **2008**, *97*, 2892.
5. "The Global Market for Advanced Wound Care Products 2014." PR Newswire, 2014 Apr 14, **2014**.
6. Paul, W.; Sharma, C. P. *Trends Biomater. Artif. Organs* **2004**, *18*, 18.
7. Stadelmann, W. K.; Digenis, A. G.; Tobin, G. R. *Am. J. Surg.* **1998**, *176*, 26S.
8. Xu, H.; Ma, L.; Shi, H.; Gao, C.; Han, C. *Polym. Adv. Technol.* **2007**, *18*, 869.
9. Jao, W. C.; Yang, M. C.; Lin, C. H.; Hsu, C. C. *Polym. Adv. Technol.* **2012**, *23*, 1066.
10. Venugopal, J.; Ramakrishna, S. *Tissue Eng.* **2005**, *11*, 847.
11. Liu, S. J.; Kau, Y. C.; Chou, C. Y.; Chen, J. K.; Wu, R. C.; Yeh, W. L. *J. Membr. Sci.* **2010**, *355*, 53.
12. Chen, J. P.; Chang, G. Y.; Chen, J. K. *Colloid Surf. A* **2008**, *313*, 183.
13. Rho, K. S.; Jeong, L.; Lee, G.; Seo, B.-M.; Park, Y. J.; Hong, S.-D.; Roh, S.; Cho, J. J.; Park, W. H.; Min, B.-M. *Biomaterials* **2006**, *27*, 1452.
14. Kumbar, S.; James, R.; Nukavarapu, S.; Laurencin, C. *Biomed. Mater.* **2008**, *3*, 034002.
15. Meng, D.; James, R.; Laurencin, C. T.; Kumbar, S. G. *IEEE Trans. Nanobiosci.* **2012**, *11*, 3.
16. Kumbar, S. G.; Nair, L. S.; Bhattacharyya, S.; Laurencin, C. T. *J. Nanosci. Nanotechnol.* **2006**, *6*, 9.
17. Schneider, A.; Wang, X.; Kaplan, D.; Garlick, J.; Egles, C. *Acta Biomater.* **2009**, *5*, 2570.
18. Barrientos, S.; Stojadinovic, O.; Golinko, M. S.; Brem, H.; Tomic-Canic, M. *Wound Repair Regen.* **2008**, *16*, 585.
19. Choi, J. S.; Leong, K. W.; Yoo, H. S. *Biomaterials* **2008**, *29*, 587.
20. Sahoo, S.; Ang, L. T.; Goh, J. C. H.; Toh, S. L. *J. Biomed. Mater. Res. A* **2010**, *93*, 1539.
21. Katti, D. S.; Robinson, K. W.; Ko, F. K.; Laurencin, C. T. *J. Biomed. Mater. Res. B* **2004**, *70*, 286.
22. Aravamudhan, A.; Ramos, D. M.; Nip, J.; Subramanian, A.; James, R.; Harmon, M. D.; Yu, X.; Kumbar, S. G. *Curr. Pharm. Des.* **2013**, *19*, 3420.
23. Papadopoulos, S.; Jürgens, K. D.; Gros, G. *Biophys. J.* **2000**, *79*, 2084.
24. Wieghaus, K. A.; Capitosti, S. M.; Anderson, C. R.; Price, R. J.; Blackman, B. R.; Brown, M. L.; Botchwey, E. A. *Tissue Eng.* **2006**, *12*, 1903.
25. Wieghaus, K. A.; Gianchandani, E. P.; Neal, R. A.; Paige, M. A.; Brown, M. L.; Papin, J. A.; Botchwey, E. A. *Biotechnol. Bioeng.* **2009**, *103*, 796.

26. Wieghaus, K. A.; Nickerson, M. M.; Petrie Aronin, C. E.; Sefcik, L. S.; Price, R. J.; Paige, M. A.; Brown, M. L.; Botchwey, E. A. *Biomaterials* **2008**, *29*, 4698.
27. Jiang, T.; Deng, M.; James, R.; Nair, L. S.; Laurencin, C. T. *Acta Biomater.* **2014**, *10*, 1632.
28. Chang, H. I.; Lau, Y. C.; Yan, C.; Coombes, A. *J. Biomed. Mater. Res. A* **2008**, *84*, 230.
29. James, R.; Toti, U. S.; Laurencin, C. T.; Kumbar, S. G. Biomedical Nanotechnology – Methods and Protocols, Sarah J. Hurst, ed., Springer: New York, **2011**; p 243–258.
30. Nada, A. A.; James, R.; Shelke, N. B.; Harmon, M. D.; Awad, H. M.; Nagarale, R. K.; Kumbar, S. G. *Polym. Adv. Technol.* **2014**, *25*, 507.
31. Harmon, M. D.; James, R.; Shelke, N. B.; Kumbar, S. G. *J. Appl. Polym. Sci.* **2013**, *130*, 3770.
32. James, R.; Toti, U. S.; Laurencin, C. T.; Kumbar, S. G. *Methods Mol. Biol.* **2011**, *726*, 243.
33. Beachley, V.; Wen, X. *Mater. Sci. Eng. C* **2009**, *29*, 663.
34. Lam, C. X.; Hutmacher, D. W.; Schantz, J. T.; Woodruff, M. A.; Teoh, S. H. *J. Biomed. Mater. Res. A* **2009**, *90*, 906.
35. Dhandayuthapani, B.; Krishnan, U. M.; Sethuraman, S. *J. Biomed. Mater. Res. A* **2010**, *94*, 264.
36. Kumbar, S. G.; Aminabhavi, T. M. *J. Appl. Polym. Sci.* **2003**, *89*, 2940.
37. Shelke, N. B.; James, R.; Laurencin, C. T.; Kumbar, S. G. *Polym. Adv. Technol.* **2014**, *25*, 448.
38. Kumbar, S. G.; Kulkarni, A. R.; Dave, A. M.; Aminabhavi, T. M. *J. Appl. Polym. Sci.* **2001**, *82*, 2863.
39. Torres-Giner, S.; Martinez-Abad, A.; Gimeno-Alcañiz, J. V.; Ocio, M. J.; Lagaron, J. M. *Adv. Eng. Mater.* **2012**, *14*, B112.
40. Zilberman, M.; Golerkansky, E.; Elsner, J. J.; Berdicevsky, I. *J. Biomed. Mater. Res. A* **2009**, *89*, 654.
41. Kumbar, S. G.; Nukavarapu, S. P.; James, R.; Nair, L. S.; Laurencin, C. T. *Biomaterials* **2008**, *29*, 4100.